Epidemiol. Infect. (2000), **124**, 295–307. Printed in the United Kingdom

Predictions of the emergence of vaccine-resistant hepatitis B in The Gambia using a mathematical model

J. N. WILSON[1]*, D. J. NOKES[2] AND W. F. CARMAN[3]

[1] *Wellcome Trust Centre for the Epidemiology of Infectious Disease, University of Oxford, OX1 3PS, UK*
[2] *Department of Biological Sciences, University of Warwick, Coventry, UK*
[3] *Institute of Virology, Church St., University of Glasgow, UK*

(*Accepted 28 October 1999*)

SUMMARY

Vaccine escape variants of hepatitis B virus (HBV) have been identified world-wide. A mathematical model of HBV transmission is used to investigate the potential pattern of emergence of such variants. Attention is focused on The Gambia as a country with high quality epidemiological data, universal infant immunization and in which escape mutants after childhood infections have been observed. We predict that a variant cannot become dominant for at least 20 years from the start of vaccination, even when using a vaccine which affords no cross protection. The dominant factor responsible for this long time scale is the low rate of infectious contacts between infected and susceptible individuals (we estimate the basic reproduction number of hepatitis B in The Gambia to be 1·7). A variant strain that achieves high prevalence will also take many years to control, and it is questionable whether emergence will be identifiable by sero-surveillance until of high prevalence. The sensitivity of the model predictions to epidemiological and demographic factors is explored.

INTRODUCTION

Hepatitis B virus (HBV) variants have been reported to arise in immunized individuals in three situations: (i) after liver transplantation, despite treatment with monoclonal antibodies against surface antigen (anti-HBs) and hyper-immunoglobulin (HBIG) treatment [1–3], (ii) neonatal infections, despite HBIG and/or vaccination in the UK [4], Italy [5], Singapore [6], Indonesia [7] and Japan [8], and (iii) horizontal infections in young children despite vaccination in The Gambia [9]. The 22 nm subviral surface antigen peptides (HBsAg) used in the current vaccines (both plasma derived and recombinant) produce a narrower immune response than immunity following infection. This has led to the possibility that a single amino acid substitution in HBsAg can allow the virus to evade the vaccine-induced immune response, allowing replication within the vaccinated individual. Several such substitutions have been reported: most commonly an arginine instead of glycine at codon 145 (G145R), but also substitutions at codons 144, 141 and 126. The evasion of vaccine induced-immunity does not always appear to be complete, however, as chimpanzees vaccinated by the standard sub-unit vaccine remained uninfected by challenge with the G145R variant [10]. This particular mutation has been identified in viruses of different genotypes suggesting it has arisen independently in different parts of the world. Indeed these variants have been identified, infrequently, in the absence of vaccination. However their emergence raises serious concern only where universal vaccination may provide an environment in which they can replace the current HBV. The WHO is currently promoting increased vaccine coverage not only in countries with high HBsAg prevalence, but world-wide [11].

This scenario provided the motivation for the

* Author for correspondence: J. N. Wilson, Department of Biological Sciences, University of Warwick, Coventry CV4 7AL, UK.

https://doi.org/10.1017/S0950268800003605 Published online by Cambridge University Press

construction and analysis of a mathematical model of the transmission of HBV, the impact of vaccination and the potential emergence of a vaccine escape variant. A mathematical model is desirable in order to identify the underlying epidemiological processes that allow a novel pathogen to be transmitted more than the wild-type and so become dominant, and also to make projections of the predicted pattern and time scale of this emergence. We focus on The Gambia as representative of those countries with high HBV transmission in Africa; one also with universal infant immunization in which the occurrence of vaccine escape mutants has been observed. The transmission dynamics of HBV in The Gambia has previously been modelled by Edmunds and colleagues [12]. We modify their model into a two-strain structure similar to the general two-strain model of acute childhood infections presented by McLean [13]. The inclusion of the age-dependent processes of transmission and carrier generation, and realistic demography, represents a significant development from that used in our preliminary studies [14].

We initially present the results of a steady state (long-term equilibrium) analysis which elucidates the conditions of vaccination coverage, cross immunity and relative transmissibility of variant to wild type, which affect the emergence of a mutant strain. We then explore the temporal patterns of emergence predicted using the age-structured, compartmental model, and assess the effect of a variety of factors on the predicted outcome, including epidemiological and demographic conditions typical of other HBV endemicity regions.

METHODS

Equilibrium model

The potential for the long term emergence of HBV variants depends both on characteristics of the vaccination programme and on the fitness of each strain at the population level, as represented by the basic reproduction number. The basic reproduction number of strain 1 and 2 (R_{01} and R_{02}) is the average number of secondary infections arising if one primary infection were introduced into a wholly susceptible population. Vaccine escape variants have not become dominant (i.e. out-competed normal HBV) prior to the introduction of HBV vaccines, suggesting the variants have a reduced replication competence. There is no direct experimental evidence of the size of this reduction, so a range of values are examined; we assume $R_{02} = \alpha R_{01}$, and examine $\alpha = 0$–1. Due to the stimulation of a broader immune response (i.e. in addition to anti-HBs) recovery from infection is assumed to produce immunity to both strains.

In a vaccinated population the competitive outcome between strains is determined by the reproduction numbers under vaccination, R_{v1} and R_{v2}. These are lower than the respective R_0's because, due to vaccination, the whole population is not susceptible. For example, an individual may make 5 potentially infectious contacts during their period of infectiousness ($R_0 = 5$), but if 3 out of every 5 people are effectively immunized then only 2 contacts will actually result in transmission ($R_v = 2$). A vaccination programme can be summarized by its coverage (ν), the vaccine-induced protection (ϕ) and the cross-immunity (c) of the vaccine. Therefore vaccine impact is ϕ against wild-type infection and $c\phi$ against variant infection. After a period under this programme, and in the absence of infection, the proportion susceptible to the wild-type (strain 1) approaches $(1-\phi\nu)$ and to the variant (strain 2), $(1-c\phi\nu)$. The reproduction numbers of strain 1 and 2 under vaccination are therefore as shown in equations (1) and (2):

$$R_{v1} = R_{01}(1-\phi\nu), \tag{1}$$

$$R_{v2} = \alpha R_{01}(1-c\phi\nu). \tag{2}$$

Elimination from a population occurs when $R_{vi} < 1$. Equations (3) and (4) show the critical vaccination coverages (ν_i'), required to reduce R_{vi} below unity and thus achieve elimination:

$$\nu_1' = \frac{1}{\phi}\left(1-\frac{1}{R_{01}}\right), \tag{3}$$

$$\nu_2' = \frac{1}{c\phi}\left(1-\frac{1}{\alpha R_{01}}\right). \tag{4}$$

By equating equations (1) and (2) we can also calculate a competitive threshold, ν_{eq}, at which point the two strains have identical reproduction numbers and would coexist (equation 5):

$$\nu_{eq} = \frac{1-\alpha}{\phi(1-\alpha c)}. \tag{5}$$

Equation (5) also provides a fairly accurate approximation of the threshold coverage for the dominance of strain 2 and the exclusion of strain 1. With values of ν greater than ν_{eq}, the vaccine escape variant has a higher reproduction number than the wild-type ($R_{v2} > R_{v1}$) and the wild-type is out-competed and does not persist. However this system of wild-type and vaccine-escape variant is not symmetrical and at

https://doi.org/10.1017/S0950268800003605 Published online by Cambridge University Press

values of ν less than ν_{eq}, the vaccine escape variant may still coexist with the wild-type. This occurs because the variant is able to infect vaccinated individuals in addition to the fully susceptible individuals who can be infected by either strain. Equation (5) therefore does not represent the threshold conditions for the persistence of strain 2 because strain 2 can persist when $R_{v1} > R_{v2}$. As discussed in the legend to Figure 2, this zone of coexistence (described by ν_2^*) can be approximated by considering the fraction of the population remaining susceptible to the variant (x_2^*) when the wild-type has infected sufficient individuals to reduce the effective reproduction number of strain 1 to unity. The thresholds describing the area of coexistence (ν_{eq} and ν_2^*), however, are only approximations and coexistence may still occur in situations in which $\nu > \nu_{eq}$ and/or $\nu < \nu_2^*$.

Dynamic model

We base our dynamic model on a deterministic, age-structured, compartmental model of HBV transmission in The Gambia developed by Edmunds and colleagues [12]. As such, our results rely on the validity of this model to accurately describe and explain wild-type HBV epidemiology. The original model was modified to accommodate a second strain – the vaccine escape variant. The two strains are assumed to act identically except in their ability to infect vaccinated individuals and in their relative transmissibility. Mathematical details of the modified model are given in the Appendix and the key elements are described in the following sections. The human population is represented by seven compartments as shown in Figure 1, and is structured by gender (g), age (a) and time (t) (Appendix (a)). The compartments represent susceptible ($X^g(a,t)$) and vaccinated ($V^g(a,t)$) individuals, individuals with primary infection of either strain 1 or 2 ($Y_1^g(a,t)$ and $Y_2^g(a,t)$), chronic carriers of strain 1 or 2 ($C_1^g(a,t)$ and $C_2^g(a,t)$) and individuals recovered from either infection ($Z^g(a,t)$). Strain 1 represents the current HBV and strain 2 a vaccine-escape variant. The population is structured by bi-monthly age-cohorts in order to include age- and gender-specific birth and death rates, age-dependent mixing rates (and resultant age-related forces of infection), and the strong age-dependence in the probability with which a primary infection may become chronic [15]. Deaths are removed from all classes at a rate, $\mu^g(a)$ which allows for specific age- and gender-stratified demographic data. Alternatively

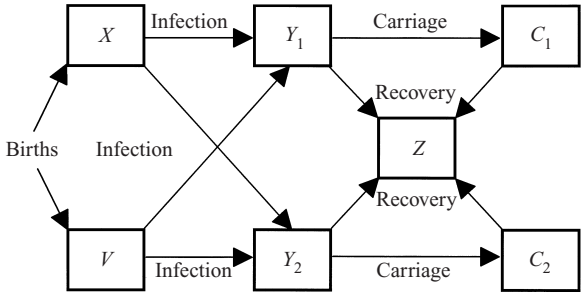

Fig. 1. Compartmental model structure with individuals susceptible (X), vaccinated (V), currently with primary HBV infection of either strain 1 or strain 2 (Y_1 and Y_2), with chronic infection of either strain 1 or strain 2 (C_1 and C_2) and those immune to re-infection by either strain (Z). Strain 1 represents the current circulating HBV strain and strain 2 the vaccine escape variant. Deaths are removed from each compartment. The vaccine is assumed to be delivered near to the time of birth, with the fraction not successfully vaccinated entering the susceptible class (X). Transmission can occur through vertical, sexual or horizontal routes. The model is age structured in order to incorporate the strong age-dependence in the probability of becoming a carrier following infection, this and other parameters are described in the text and Appendix.

type I or II mortality schedules can be accommodated (type I mortality assumes all individuals survive until the average expectancy of life (L), type II mortality assumes individuals die at a constant death rate equivalent to $1/L$ [16]). There is no infection-induced mortality. Births enter the youngest male and female age-cohort at a rate $m(a)$ dependent on the number of females of child-bearing age and assuming a 1:1 sex-ratio of births. We assume no maternally derived antibody protection in the new-born. A fraction (ν) of births enter the vaccinated class and the remainder ($1-\nu$) enter the susceptible class (see Appendix (b)).

Transmission

The infectious population is calculated as the sum of primary infections and carriers, $Y_s^g(a,t) + \eta C_s^g(a,t)$, for each strain s; the reduced viral load of carriers (C) is assumed to make them less infectious than acute cases (Y) by a factor η. This method is consistent with Edmunds and colleagues [12] and is chosen in preference to that of McLean & Blumberg [17], in which e-antigen-positive ($HBeAg^+$) carriers are assumed to be fully infectious and $HBeAg^-$ carriers uninfectious. The per capita rates at which susceptibles of one or other sex become infected by one or other strain (the forces of infection, $\lambda_s^g(i,t)$), are a function of the size of this infectious population which mix with the susceptibles of each age class i. They are

https://doi.org/10.1017/S0950268800003605 Published online by Cambridge University Press

Table 1. *Summary of model parameters*

Symbol	Parameter	Base-line parameter estimates	References
$N^g(a,t)$	Present population size	748000 (The Gambia)	[23]
$\mu^g(a)$	Death rate for gender (g) and age (a)	Table 3	[23]
$m(a)$	Birth rate of females of age a	Table 3	[23]
α	Relative transmission coefficients of strains	0·9	No data
κ	Sexual transmission coefficient for strain 1 ($\alpha\kappa$ for strain 2)	0·574 per partnership	[12]
ϕ^m	Rate of partner change	2·3 per year (male) (female rate modified for changes in sex ratio, see Appendix (c))	[12]
b	Vertical transmission coefficient for strain 1 (αb for strain 2)	0·71	[12]
$p(a)$	Probability of becoming a carrier	0·885 for $a = 0$–6 months $\exp(-0{\cdot}645\, a^{0{\cdot}455})$ for $a > 6$ months	[15]
η	Relative infectiousness of chronic and primary infection	0·16	[12]
γ	Recovery rate (acute)	4·8 per year (average duration 2·5 months)	[12]
σ	Recovery rate (chronic)	0·023 per year (average duration 43·5 years)	[12]
Q	Mutation probability	0·001 per infection	[18, 26]
ν	Proportion of population covered by vaccination programme	0·8	
ϕ	Degree of vaccine-induced protection	0·9	[20]
c	Cross-immunity of vaccine	0·5	No data
$\lambda_s^g(i,t)$	Force of infection (per person incidence)	see Appendix (d)	[12]

calculated for horizontal (parenteral) and sexual transmission for ages over 15 years and as horizontal transmission alone for ages under 15. Horizontal transmission is modelled by a density-independent term i.e. of the form $\beta I/N$, where I is the infectious population, N is the total population and β is a matrix which determines the pattern of mixing between the different age-groups of susceptible and infectious individuals and the probability of transmission following contact (see Anderson and May, [16]). Sexual transmission is also modelled by a density-independent term though with age-independent, heterosexual mixing between susceptibles and infectious individuals over 15 years old. These terms are presented in full in Appendix (c). The model could be simplified by amalgamating horizontal and sexual transmission but we retain the distinction to be consistent with the model of Edmunds and colleagues [12].

To accommodate a second strain the forces of infection due to normal virus or its mutated variant are modified by a mutation term Q, in a similar way to McLean and Nowak [18]. Q is the probability that an infectious contact with strain 1 results in an infection with strain 2, and vice versa. Thus the total force of infection (Λ) due to strain s acting on susceptibles (of sex g and age a) is defined as:

$$\Lambda_s^g(a,t) = (1-Q)\,\lambda_s^g(a,t) + Q\lambda_{s'}^g(a,t), \qquad (6)$$

in which $\lambda_s^g(a,t)$ is the force of infection for strain 1 or 2 of which a proportion $(1-Q)$ have not mutated and $\lambda_{s'}^g(a,t)$ is the force of infection for the alternative strain of which a proportion Q have mutated. Vaccination can also be thought to modify the forces of infection. The degree of protection of the vaccine against strain 1 is ϕ and against strain 2, $c\phi$ [19]. Thus c is a cross-immunity term reflecting the relative protection of the vaccine against strain 2. The vaccinated class remain partly susceptible to infection, but experience a force of infection reduced by a factor $(1-\phi)$ for strain 1 and by $(1-c\phi)$ for strain 2.

Vertical or perinatal transmission is modelled by a fraction (b) of births from the infectious population of each strain, entering the primary infection class of the youngest age-cohorts; b is assumed to be affected by mutation and vaccination in the same way as horizontal and sexual transmission (see Appendix (b)).

Recovery

Individuals were assumed to recover from primary infection at a rate γ and from chronic infection at a rate σ, for both strains, where $\gamma \gg \sigma$. The probability that a primary infection becomes chronic is modelled by an exponentially declining age-dependent function $p(a)$ as described in Edmunds and colleagues [15] and summarized in Table 1. Recovery from primary and

https://doi.org/10.1017/S0950268800003605 Published online by Cambridge University Press

Table 2. *Demographic parameters for The Gambia* [23]

Age (a years)	Initial population size (thousands)*		Death rates		Birth rates
	$N^f(a,0)$	$N^m(a,0)$	$\mu^f(a)$	$\mu^m(a)$	$m(a)$
< 1	13·4	13·2	0·184	0·215	0·000
1–4	53·6	52·8	0·028	0·024	0·000
5–9	51·0	52·0	0·049	0·044	0·000
10–14	42·0	42·0	0·042	0·044	0·000
15–19	36·0	35·0	0·033	0·038	0·200
20–24	33·0	32·0	0·021	0·022	0·293
25–29	30·0	29·0	0·019	0·019	0·285
30–34	25·0	26·0	0·033	0·022	0·222
35–39	21·0	24·0	0·035	0·018	0·161
40–44	17·0	20·0	0·041	0·033	0·077
45–49	14·0	16·0	0·040	0·044	0·040
50–54	12·0	13·0	0·034	0·043	0·000
55–59	9·0	9·0	0·053	0·068	0·000
60–64	7·0	7·0	0·054	0·058	0·000
65–69	5·0	4·0	0·067	0·102	0·000
70–74	2·0	2·0	0·161	0·139	0·000
75–80	0·0	0·0	0·467	0·469	0·000

* f, female; m, male.

chronic infections is again assumed to produce immunity to reinfection by either strain.

Parameter estimation

The efficacy of the current HBV vaccine against the normal HBV type has been estimated in The Gambia to be between 93% and 956% [20]. The values are chosen to represent an estimate of the 'degree' of protection (ϕ) of the vaccine, setting $\phi = 0{\cdot}9$, which measures the reduction in the force of infection experienced by vaccinees [19]. If the vaccine affords the same degree of protection against the variant as against normal HBV, the cross-immunity term, c, would be equal to 1; if half as much protection then $c = 0{\cdot}5$; and if the vaccine provides no cross-protection then $c = 0$. We examine universal infant vaccine programmes with coverage ν, in which the vaccine is assumed to 'take' in all vaccinated individuals (i.e. we ignore the small proportion who do not seroconvert) and in which the 'degree' of protection is assumed not to wane [21].

Edmunds and colleagues [12] estimated the age- and gender-stratified birth and death rates for The Gambia [23] and the rates of recovery from acute and chronic HBV infection. The probability of becoming a carrier was estimated by Edmunds and colleagues [15]. The model's parameters are summarized in Tables 1 and 2. Edmunds and colleagues [12] also estimated the force of infection in different age-groups from serological data from The Gambia. These estimates allow the calculation of the transmission matrices (β) as discussed in Anderson and May [24]. For the purposes of estimating age-specific effective contact rates it is necessary to discretize age into n classes from the n estimates of the force of infection. Edmunds and colleagues [12] showed that five age classes were sufficient to capture the epidemiology of HBV in The Gambia. The pattern of mixing chosen is also consistent with the pattern used by Edmunds and colleagues [12]: this assumes equal levels of transmission among and between one age group and all younger age groups. Thus transmission within the youngest age group (0–1 year olds) has a unique value, whilst adults (over 15 years old) are assumed to mix (non-sexually) with all the other age groups equally. Matrices for realistic population growth and stationary population situations are shown in Appendix (d).

Model implementation and output

The system of partial differential equations was coded in FORTRAN and solved under the parameter values given in Table 1 using a Sun processor (with a time step of 1 day). Vaccination was assumed to occur once the model had settled to equilibrium (after 200 years). If a population grows in size, the proportions of individuals in each age cohort change. Thus for

https://doi.org/10.1017/S0950268800003605 Published online by Cambridge University Press

simulations of a growing population in The Gambia the model was run to equilibrium without vaccination to determine the proportions of individuals in each infection class, these proportions were scaled to the known present-day age-distribution of The Gambia and vaccination introduced at time zero.

The incidence of each strain per 100000 people was calculated as the force of infection, $\Lambda_s^g(a,t)$, multiplied by the total susceptible population (including vaccinees), summed over one year (t) across all ages (a) and for both genders (g), as a proportion of the total population $N^g(a,t)$, scaled to 100000.

Incidence of strain s per 100000 per year =

$$\Sigma_t \Sigma_a \Sigma_g \Lambda_s^g(a,t)\,[X^g(a,t)+(1-c\phi)V^g(a,t)] \times \frac{100000}{\Sigma_t \Sigma_a \Sigma_g N^g(a,t)} \quad (7)$$

(where $c = 1$ for strain 1).

The prevalence of carriers at time t was calculated as the sum of the carrier classes across all ages and both genders as a proportion of the total population.

$$\text{Prevalence of carriers of strain } s \text{ at time } t = \frac{\Sigma_a \Sigma_g C_s^g(a,t)}{\Sigma_a \Sigma_g N^g(a,t)} \quad (8)$$

RESULTS

The results of the study are in two parts. Initially the long term equilibrium or steady state results are examined (i.e. many years after the introduction of a vaccination programme) before looking at the temporal dynamics prior to equilibrium using the age- and time-structured model described above.

Equilibrium model analysis

Analysis of the equilibrium model involves (i) estimating an R_0 for wild-type HBV infection (ii) estimating the degree of protection (ϕ) of the vaccine against the wild-type and then (iii) exploring the effect of different values of cross-immunity (c), coverage (ν) and relative transmissibility (α). Edmunds [25] estimates $R_0 = 5$ using an *age-independent* model of serological HBV data in The Gambia. The same data described by an *age-dependent* model will have a lower R_0 as the force of infection and the probability of carriage decreases in older age groups [16]. In the results of our age-dependent model we estimate R_0 to be approximately 1·7 and we therefore use this estimate in the equilibrium analysis. The precise calculation of R_0 for our dynamic model is beyond the scope of this paper.

The conditions defined by equations (3) and (4) (assuming $\phi = 0{\cdot}9$ and $R_{01} = 1{\cdot}7$), produce the graphs in Figure 2*a* and *b*. It is clear from these graphs that both strains are only eliminated at high levels of coverage (ν) and cross-immunity (c). At higher α and hence higher R_{02} (Fig. 2*a*) the variant is able to outcompete the normal HBV under a greater range of parameters. At lower α (Fig. 2*b*), R_{02} is lower and so strain 2 can be eliminated with lower coverage and with a less cross-protective vaccine. Thus there is a balance between the advantage to the variant of the vaccination programme subduing the normal HBV (its competitor) and the possibility that the vaccination eliminates the variant as well.

Although reproduction numbers can largely determine the eventual pattern of dominance, they are not indicative of the time-scale or magnitude of the emergence of a variant. This is determined by the rate at which susceptibles to strain 1 and 2 accumulate. Individuals susceptible to the variant include both unvaccinated and vaccinated individuals in whom the vaccine is, to a greater or lesser degree (as defined by c) ineffective. The incidence of the variant infections cannot increase until the susceptible threshold is crossed ie. the effective reproduction number exceeds unity (the respective threshold proportions are $1/R_{01}$ and $1/R_{02}$ [16]). From then the rate of spread will be determined by the transmission coefficients, i.e. the rates of effective contacts within and between age classes in the population.

Dynamic model analysis

The results of the age-structured model are presented in Figures 3–6. Figure 3*a* shows the projected incidence of normal HBV and vaccine escape variant infections through time after vaccination in The Gambia, at different values of vaccine cross-immunity (c), with vaccine coverage at 80%. If $c = 0$ then the variant becomes dominant, achieving an incidence equivalent to the normal HBV strain (reduced by a factor approximately equal to α, the ratio of the reproductive capacities of the two strains, R_{02}/R_{01}) under the baseline model and parameter assumptions. If $c > 0{\cdot}4$ then both strains are eliminated.

In Figure 3*b* the vaccine coverage is varied from 0 to 100%, with a fixed cross-immunity term ($c = 0{\cdot}5$), and the equilibrium prevalence of carriers (after 1000

https://doi.org/10.1017/S0950268800003605 Published online by Cambridge University Press

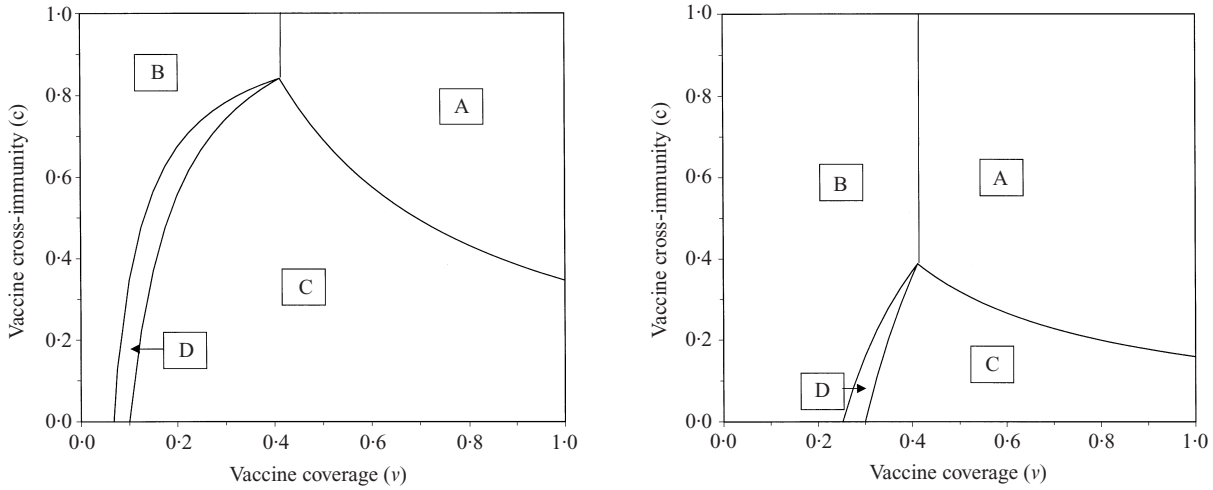

Fig. 2. Four equations (ν'_1, ν'_2, ν_{eq} and ν^*_2) determine four potential outcomes of vaccination: wild-type and variant eradicated (A), wild-type (B), or variant (C) exist alone or both strains coexist (D). The elimination thresholds (ν'_1 and ν'_2) are calculated for wild-type and vaccine-escape variant respectively in a vaccinated population where coverage is ν and the impact of the vaccine is ϕ ($\phi = 0{\cdot}9$) against the wild-type (strain 1) and cϕ against the variant (strain 2). These are assumed to be 'all or nothing' protection parameters. For example when $c = 0{\cdot}5$ the vaccine is half as effective against the variant as it is against the wild-type. A competitive threshold is approximated by ν_{eq}, which also acts as a persistence threshold for the wild-type. An area of coexistence is approximated by considering the fraction of the population remaining susceptible to the variant (x^*_2) when the wild-type has infected sufficient individuals to reduce the effective reproduction number of strain 1 to unity. Thus a fraction $x^*_1 = 1/R_{01}$ are susceptible to wild-type infection (and to the variant) and a further $(1-c)\phi\nu$ are susceptible to the variant only. Thus $x^*_2 = 1/R_{01} + (1-c)\phi\nu$. By setting $R_{02}x^*_2$ equal to unity we can calculate a threshold vaccination coverage for the persistence of the variant: $\nu^*_2 = (1-\alpha)/\alpha R_{01}\sigma(1-c)$. R_{01} is assumed to be 1·7 and $R_{02} = \alpha R_{01}$, i.e. the relative transmissibility of wild-type to variant is α: (*a*) $\alpha = 0{\cdot}9$, (*b*) $\alpha = 0{\cdot}5$.

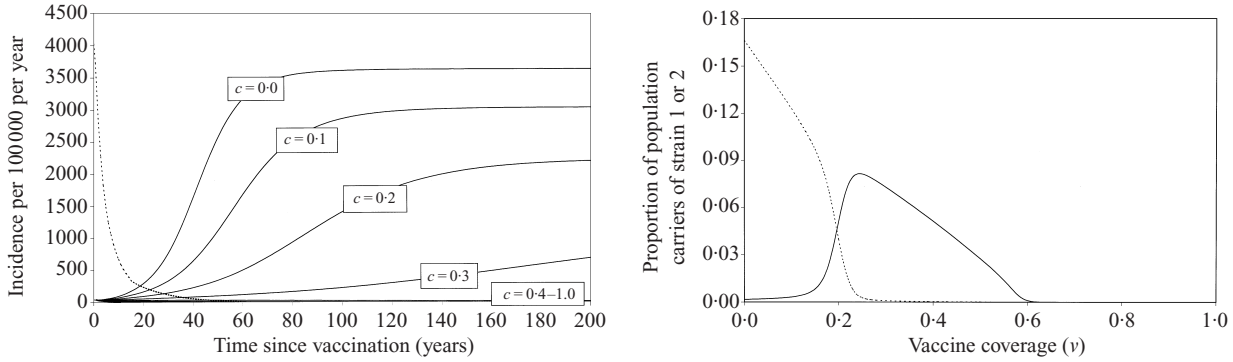

Fig. 3. (*a*) The predicted incidence of HBV infection per 100000 per year (as calculated by equation (7)) after a vaccination programme with 80% coverage introduced at time zero when infection is at a stable equilibrium (under baseline parameter settings, Table 1). The vaccine was assumed to provide 90% protection against the normal HBV strain ($\phi = 0{\cdot}9$). The protection against the variant was reduced by a factor c, and the different lines describe simulations with c varying from 0 to 1. The dotted lines represent the normal HBV and the solid lines represent the variant, with values of c decreasing from the lower line upwards, all other parameters are base-line. Even with a vaccine which afforded no cross-protection ($c = 0$) the variant is predicted not to become dominant for over 20 years. (*b*) The predicted prevalence of carriers at equilibrium (i.e. the steady state prevalence following many years of vaccination, as calculated by equation (8)) at different vaccine coverage levels, with all other parameters base-line. The dotted line represents the normal HBV and the solid line represents the vaccine escape variant. The cross-protection term (c) was assumed to be 0·5. The variant achieves dominance at intermediate coverage levels but is eliminated at high coverage levels.

years) is plotted. The variant achieves dominance at intermediate levels of coverage being itself eliminated at high coverage levels (as in Fig. 2). For higher and lower values of c (i.e. greater or less cross-immunity) the peak prevalence of strain 2 shifts, aligning with higher or lower coverage levels respectively; predictably this peak is higher at low values of c and lower when cross-immunity is high.

https://doi.org/10.1017/S0950268800003605 Published online by Cambridge University Press

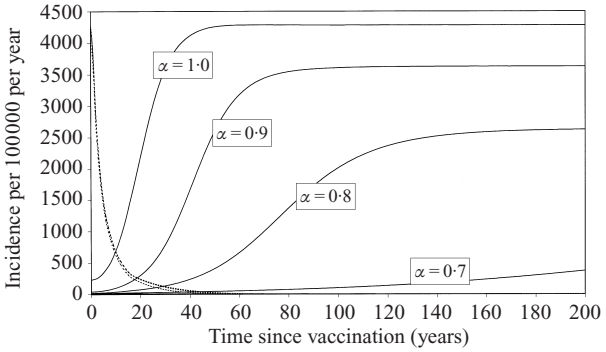

Fig. 4. The predicted incidence per 100000 per year for different values of α, the relative transmissibility of variant to wild-type HBV. The solid lines represent the variant at different values of α. The lower dotted line represents the wild-type when $\alpha = 1{\cdot}0$, the other dotted line represents the wild-type at all other values of α. When $\alpha = 1{\cdot}0$ the incidence of wild-type is lower and the incidence of variant is higher at time = 0 than for other simulations, hence the slightly more rapid elimination. With $\alpha = 1{\cdot}0$ the variant would eventually attain equal incidence to the wild-type, but vaccination is introduced before this equilibrium is reached. At values of $\alpha \leqslant 0{\cdot}6$ the variant does not emerge. (coverage, $\nu = 0{\cdot}8$; cross-immunity, $c = 0{\cdot}0$; other parameters base-line).

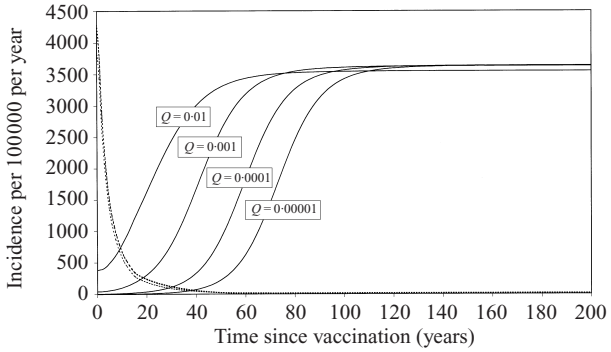

Fig. 5. The predicted incidence per 100000 per year for different values of Q, the probability of an infection with strain 1 resulting in an infection with strain 2 and vice versa, i.e. the chance of mutation per infection. The solid lines represent the variant at different values of Q. The lower dotted line represents the variant when $Q = 0{\cdot}01$, the other dotted line represents the variant at all other values of Q. The equilibrium prevalence of the variant before vaccination (time < 0) is significantly higher with high mutation rates ($Q = 0{\cdot}01$), and this reduces the time-scale of emergence of the variant after vaccination as well as reducing the time-scale for the elimination of the wild-type. (coverage, $\nu = 0{\cdot}8$; cross-immunity, $c = 9{\cdot}9$; relative transmissibility $\alpha = 0{\cdot}9$; other parameters base-line).

Sensitivity

The dynamics of the original model [12, 25] appear relatively robust to realistic parameter variation, e.g. recovery rates (σ and γ), the relative infectiousness of acute and carriers (η) and the form of the transmission matrix (β). We explore the predicted patterns of emergence of vaccine escape variants under different values of the parameters describing the relative transmissibility of the variant (α), the mutation term (Q) and the demographic parameters (birth and death rates).

Relative transmissibility

The relative transmissibility of wild-type and variant (α) influences the force of infection of the variant. Figure 4 shows model simulations at different values of α. In this scenario if $\alpha \geqslant 0{\cdot}7$ the variant emerges to a steady state the magnitude of which is lower at lower values of α. If $\alpha \leqslant 0{\cdot}6$ the variant does not emerge at all even though $\nu = 0{\cdot}8$ and $c = 0{\cdot}0$. The simulation when $\alpha = 0{\cdot}6$ therefore provides a method to estimate R_{01}. The simulation is on the threshold of emergence suggesting R_{v2} is close to unity, hence, with $R_{v2} = 1$, $\alpha = 0{\cdot}6$ and $c = 0{\cdot}0$, we can estimate $R_{01} = 1/0{\cdot}6$ (equation (2)). Therefore we use $R_{01} = 1{\cdot}7$ in the equilibrium analysis. Differences between the dynamic model predictions and those of the equilibrium analysis may arise as the estimate of $R_{01} = 1{\cdot}7$ is an approximation. Furthermore the equilibrium analysis does not make predictions of steady state incidence. The simulation with $\alpha = 1{\cdot}0$, i.e. when the variant has the same force of infection (and basic reproduction number) as the wild-type, differs from the other simulations in Figure 4 because the prevalence of the variant has not reached equilibrium (after 200 years) when the vaccination programme starts (see time = 0, Fig. 4). Indeed this could be the situation with one or more of the HBV variants observed today; the particular mutation may have occurred long ago, allowing vaccine escape of equivalent transmissibility to normal HBV (i.e. equivalent viral replication), yet the variant has still not attained equal prevalence by the time the vaccination programme starts. An estimate of the relative transmissibility of wild-type and variant is thus required.

Mutation term

The mutation term, Q, was set at 0·001 i.e. 1 in every 1000 infections with wild-type HBV results in infection with the variant and vice versa. It is difficult to estimate this population level term from the mutation rate of individual viruses (an estimate from the hepadnaviridae is 2×10^{-4} base substitutions per site

https://doi.org/10.1017/S0950268800003605 Published online by Cambridge University Press

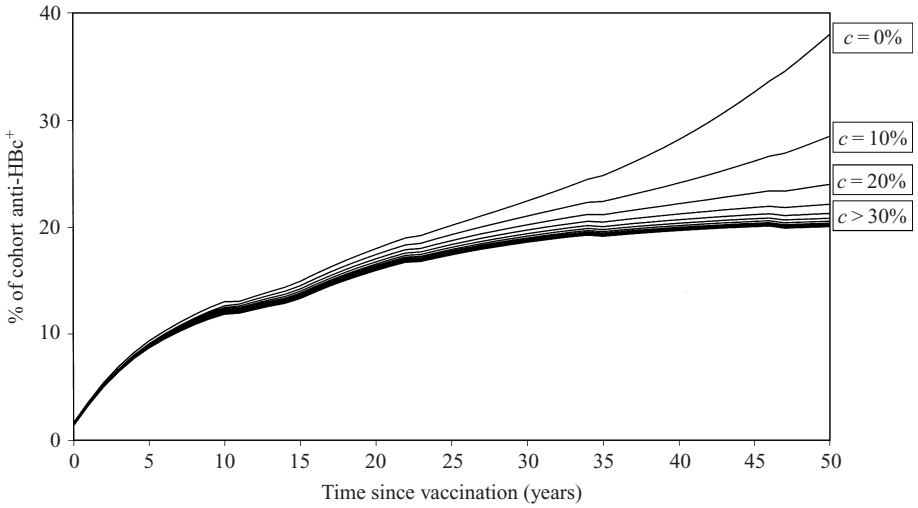

Fig. 6. The predicted prevalence of anti-HBc in the first year vaccinated cohort in The Gambia. We assume all classes in Fig. 1 are anti-HBc positive except susceptible (X) and vaccinated individuals (V). The different lines represent simulations with the cross-protection term, c, varied from 0 to 1. The graph shows that a serological survey may not be able to discriminate between values of c for 30–40 years after vaccination begins. The projected lines are not smooth as the cohort progresses through different mortality age brackets, see Table 2 (coverage, $\nu = 0{\cdot}8$; relative transmissibility $\alpha = 0{\cdot}9$; other parameters base-line).

per year [26]), in particular expressing the number of variant virions in terms of infectiousness. But by varying Q within a wide range, ie. 0·00001 and 0·01, (all other parameters are base-line with $c = 0{\cdot}0$) the rise in incidence is transposed approximately 15 years earlier for each tenfold rise in the mutation rate (see Fig. 5). The transition from one strain to another (as in Fig. 3*b*) becomes more gradual if the mutation rate is higher. Similar results can be produced by setting Q to zero and introducing an equivalent equilibrium number of individuals infected with the variant at the beginning of the vaccine programme. Thus the mutation term is important in determining the number of people infected with the variant at the beginning of the vaccine programme but less so once the epidemic is underway. The model is very sensitive to this initial prevalence and stochastic events may be important at these low prevalence levels.

Birth and death rates

Simulations using realistic age-dependent birth and death rates (yielding a $\sim 3\%$ annual population growth rate in The Gambia) were compared with simulations using a type II schedule (constant age-independent rate of 0·025 for births and deaths and, as birth rate equals death rate, zero population growth). The simulations produced qualitatively similar but quantitatively different results. Under high population growth, the proportion of the population in the younger age classes increases, thus increasing the proportion of the population at high risk of infection and carriage. In consequence the incidence and prevalence of HBV is higher in these situations and the emergence of a variant predicted to be faster than within a slowly growing or stationary population.

Detection of variants by serological survey

From these results it appears that the most significant unknown parameter in The Gambia is the cross-immunity of the vaccine (c) which determines the protection of the present vaccine against the dominant variant, (though relative transmissibility is also important). Vaccine efficacy crucially needs to be evaluated now in order to determine whether vaccine modifications are required. Figure 6 shows projections for the prevalence of anti-HBc observable in those individuals vaccinated at birth in the first year of The Gambian vaccination programme (with baseline parameters and different values of c). The model therefore follows a single age-cohort for 50 years and predicts the fraction of the cohort that would be positive for anti-HBc. This cohort is chosen as it is likely to be the first to show signs of break-through infections due to poor vaccine cross-immunity. We assume all individuals who are or have been infected, by either strain, are positive for anti-HBc. The predictions seen in Figure 6 show that different levels of vaccine-induced cross-immunity (c) cannot be

https://doi.org/10.1017/S0950268800003605 Published online by Cambridge University Press

easily distinguished for at least 30 or 40 years after the start of vaccination. This long time-scale results partly from the slow accumulation of people susceptible to the variant and partly from the inherently low rate of transmission of HBV. The emergence of a vaccine escape variant, and a measurement of c, may thus remain essentially hidden from anti-HBc serosurveillance for a number of decades. This result argues for the use of highly specific assays, such as Polymerase Chain Reaction based techniques, in the surveillance of populations for escape variants.

DISCUSSION

Conditions for emergence

This paper has examined the parameters which determine whether, and how, a vaccine escape variant of HBV will emerge. The characteristics of the vaccine programme and the reproductive potential of the viruses will together determine whether the variant will be transmitted more than the normal HBV (Fig. 2) and whether either or both strains will persist. A comparison between Figure 2*a* (when $c = 0{\cdot}8$) and Figure 3*b* reveals there is a considerable amount of coexistence around the transition area from one strain to another which is not altogether predicted in Figure 2*a*. The equilibrium analysis assumes $Q = 0{\cdot}0$, which may be why the transition is more tightly constrained. Previous mathematical models have been used to describe coexistence in situations with super-infection [27], strong density-dependent host-mortality [28] and cross-species infection. Situations in which prior infection with the virulent, wild-type strain is required for infection by the variant, may also produce cycling and hence a dynamic coexistence of strains [29].

Time scale of emergence

The analysis of effective reproduction numbers offers limited insight; the *pattern* of emergence will be determined by the rate at which susceptible individuals accumulate and by the magnitude of the transmission coefficients and the particular demography and transmission scenario in question. The results from the dynamic model differ from those of McLean [13] as strain 2 emerges monotonically over a long time period, rather than as oscillatory epidemics. Although HBV is highly contagious at the individual level, i.e. there is a high probability of transmission per infectious contact, the rate of such contacts is low. Thus, even once the susceptibles (including vaccinated individuals) have attained threshold levels, the time-scale of emergence is in the order of decades, in contrast to solely acute infections such as influenza, where the time-scale of emergence may be in the order of months or weeks. Another consideration is the persistence of the pool of carriers infected by the wild-type virus, these remain in competition with the variant for susceptibles for many years, thus further reducing the rate of emergence. The slow emergence is also exaggerated because HBV variants are thought only to evade vaccine-induced immunity whilst it appears many influenza variants, for example, can also evade infection-induced immunity, hence the accumulation of individuals susceptible to HBV variants will be slower than for influenza variants. It should also be noted that the estimate of HBV $R_0 = 1{\cdot}7$ is very low relative to infections such as measles and influenza, as well as being dominated by the duration of infectiousness component rather than the contact rate. The chronic nature of the infection suggests that if an HBV variant is allowed to achieve high prevalence (i.e. one noticeable from a serological survey) it will take many decades to eliminate, even if a more cross-reactive vaccine is introduced in the future.

Sensitivity

The main result of this study depends on the characteristic low transmission coefficient and long average duration of infectiousness of HBV and is thus robust to inaccuracies in other parameter estimates. The disease relies on long term infections producing new cases at a relatively low rate; hence variants will emerge slowly and, if allowed to accumulate, will also take a long time to eradicate. This is true even in The Gambia where the force of infection is high and where a youthful, growing population is suggested to speed the spread of an HBV variant. In other parts of the world, such as S.E. Asia, vertical transmission is thought to be the dominant route by which individuals become carriers. This is related to the strong age-dependence in the probability of becoming a carrier and the higher proportion of HBeAg positive carrier mothers in S.E. Asia compared to, for example, Sub-Saharan Africa. However pre-vaccination Taiwan appears to have had the highest known incidence of perinatal transmission, yet it has been estimated that more than 60% of carriers were infected horizontally [25]. Moreover if population growth is low and families have on average only two children then it can

https://doi.org/10.1017/S0950268800003605 Published online by Cambridge University Press

be seen that vertical transmission alone can never produce a R_0 greater than unity. Vertical transmission is therefore expected to be more important in the emergence of a variant in rapidly growing populations. Most cases of HBV vaccine escape have been reported in neonates (though this may be a reporting bias). Serological studies show vertical infection is a minor transmission route in The Gambia compared to horizontal transmission and model simulations show that even if the probability of transmission from carrier mother to infant (b) is high, this has little impact on the dynamics of the emergence of a variant (results not shown). Data were not available to model the precise effect of vertical transmission in S.E. Asia. Age-stratified serological surveys (prior to vaccination) are required to measure the proportion of the population which is infected vertically (i.e. HBsAg positive or HBcAg positive at birth) and provide an estimate of the force of horizontal infection and hence the relative importance of the vertical and horizontal routes in these areas.

It appears that the magnitude or force of horizontal infection in The Gambia is the lower limiting factor in the time-scale of the emergence of a vaccine escape variant. High endemicity countries clearly represent situations in which emergence will be most rapid. In intermediate and low endemicity countries the force of horizontal infection will be lower and hence the rate of emergence will be slower. The large number of susceptible individuals in intermediate and low endemicity countries might be predicted to increase the rate of spread of a variant, but the underlying infectious contact rate (reflected in the transmission rates) is so low that this is unlikely to be the case. In countries with type I mortality (i.e. low infant and adult mortality until close to the average life expectancy L), ageing populations and slow population growth combine to produce proportionally fewer individuals in the high-risk, young-age groups, thus reducing the prevalence of HBV carriers, the incidence of infection and hence reducing the potential rates of spread of variants.

Serological surveillance

The model suggests that anti-HBc serological surveys of the first vaccinated cohort of neonates in The Gambia may be unable to determine the effectiveness of the vaccine against the variant for 30–40 years. If assays for HBsAg are unable to detect all HBV variants, carriers may accumulate undetected (except through polymerase chain reaction based techniques) and continue to remain a source of infection for decades, with significant cost implications for undeveloped countries. Consequently it may be prudent to err on the side of caution and assume that the current vaccines are not sufficiently cross-reactive.

The key areas for development should therefore include (i) an estimation of the cross-immunity of the vaccine, (ii) estimation of the relative transmissibility of variant and wild-type (for example by measuring relative rates of viral replication), (iii) the development of surveillance strategies capable of detecting emergent variants at an early stage and (iv) the development and implementation of vaccines designed with a reduced risk of selecting for variants: probably with a wider epitope range specifically inducing neutralizing antibodies against the commonest vaccine-associated variants.

ACKNOWLEDGEMENTS

We thank Dr W. J. Edmunds, Dr N. M. Ferguson and Dr D. J. Austin for critical comments and technical assistance. D.J.N. was supported by the Royal Society and J.N.W. was in receipt of an MRC studentship.

APPENDIX. SUMMARY OF MODEL EQUATIONS (SEE TEXT FOR DETAILS)

(a) System of partial differential equations

$$\frac{\partial X^g(a,t)}{\partial a}+\frac{\partial X^g(a,t)}{\partial t}=-X^g(a,t)\,(\mu^g(a)+\Lambda_1^g(a,t)+\Lambda_2^g(a,t))$$

$$\frac{\partial V^g(a,t)}{\partial a}+\frac{\partial V^g(a,t)}{\partial t}=-V^g(a,t)\,(\mu^g(a)+(1-\phi)\,\Lambda_1^g(a,t)+(1-c\phi)\,\Lambda_2^g(a,t))$$

$$\frac{\partial Y_1^g(a,t)}{\partial a}+\frac{\partial Y_1^g(a,t)}{\partial t}=(X^g(a,t)+(1-\phi)\,V^g(a,t))\,\Lambda_1^g(a,t)-(\mu^g(a)+\gamma)\,Y_1^g(a,t)$$

https://doi.org/10.1017/S0950268800003605 Published online by Cambridge University Press

$$\frac{\partial Y_2^g(a,t)}{\partial a}+\frac{\partial Y_2^g(a,t)}{\partial t}=(X^g(a,t)+(1-c\phi)\,V^g(a,t))\,\Lambda_2^g(a,t)-(\mu^g(a)+\gamma)\,Y_2^g(a,t)$$

$$\frac{\partial C_1^g(a,t)}{\partial a}+\frac{\partial C_1^g(a,t)}{\partial t}=p(a)\,\gamma\,Y_1^g(a,t)-(\mu^g(a)+\sigma)\,C_1^g(a,t)$$

$$\frac{\partial C_2^g(a,t)}{\partial a}+\frac{\partial C_2^g(a,t)}{\partial t}=p(a)\,\gamma\,Y_2^g(a,t)-(\mu^g(a)+\sigma)\,C_2^g(a,t)$$

$$\frac{\partial Z^g(a,t)}{\partial a}+\frac{\partial Z^g(a,t)}{\partial t}=(1-p(a))\,\gamma(Y_1^g(a,t)+Y_2^g(a,t))+\sigma(C_1^g(a,t)+C_2^g(a,t))-\mu^g(a)\,Z^g(a,t)$$

(b) Birth terms

The birth terms (including vaccination, vertical transmission and mutation) entering the youngest age-cohorts of classes X, V, Y_1 and Y_2 are shown below; the sex ratio is assumed to be 1:1, i.e. half the births are male and half female.

$$X^g(1,t)=\tfrac{1}{2}\sum_a m(a)(1-\nu)\{N^f(a,t)-b[Y_1^f(a,t)+\alpha Y_2^f(a,t)+\eta(C_1^f(a,t)+\alpha C_2^f(a,t))]\}$$

$$V^g(1,t)=\tfrac{1}{2}\sum_a m(a)\,\nu\{N^f(a,t)-b[(1-\phi)\,(Y_1^f(a,t)+\eta C_1^f(a,t))+(1-c\phi)\,(Y_2^f(a,t)+\eta C_2^f(a,t))]\}$$

$$Y_1^g(1,t)=\tfrac{1}{2}\sum_a m(a)\,b\{(1-\phi\nu)\,(Y_1^f(a,t)+\eta C_1^f(a,t))\,(1-Q)+(1-c\phi\nu)\alpha\,(Y_2^f(a,t)+\eta C_2^f(a,t))\,Q\}$$

$$Y_2^g(1,t)=\tfrac{1}{2}\sum_a m(a)\,b\{(1-c\phi\nu)\alpha\,(Y_2^f(a,t)+\eta C_2^f(a,t))\,(1-Q)+(1-\phi\nu)(Y_1^f(a,t)+\eta C_1^f(a,t))\,Q\}$$

(c) Transmission terms

The horizontal (π) and sexual (ρ) transmission components of the force of infection, λ, are shown below:

$$\lambda_s^g(i,t)=\pi_s^g(i,t)+\rho_s^g(i,t)$$

$$\pi_s^g(i,t)=\frac{\Sigma_{j=1}^{5}[\beta_s(i,j)\,\Sigma_{a=\mathrm{age}(j)+1}^{\mathrm{age}(j+1)}\{Y_s^f(a,t)+Y_s^m(a,t)+\eta(C_s^f(a,t)+C_s^m(a,t))\}]}{\Sigma_{a=1}^{480}\{N^f(a,t)+N^m(a,t)\}}$$

$$\rho_s^g(i,t)=\frac{k_s\,\phi^g(i)\,\Sigma_{a=91}^{480}\,Y_s^{g'}(a,t)+\eta C_s^{g'}(a,t)\}}{\Sigma_{a=91}^{480}\,N^{g'}(a,t)},\quad \text{for } i=5,\ \text{otherwise } \rho_s^g(i,t)=0.$$

The function age(j) corresponds to the age-class upper limits, in years, of the five age classes used in (Appendix (d)) expressed as bimonthly cohorts with a maximum life expectancy of 80 years (i.e. a = 1–480). The gender g' represents the alternate gender to g. Sexual transmission is assumed only to occur in those over 15 years old ($a > 90$; $i = 5$). The rate of partner change for each gender g is ϕ^g. The female rate is adjusted to compensate for changes in sex ratio caused by the different age-dependent death rates of males and females [12]. The per partnership rate of transmission is k_1 for wild-type HBV (strain 1). Both the sexual and horizontal transmission of the variant is reduced by α, so $k_2=\alpha k_1$ and $\beta_2(i,j)=\alpha\beta_1(i,j)$. The overall force of infection, $\lambda_s^g(i,t)$, is modified by mutation as shown in equation (6).

(d) 'Who acquires infection from whom' and force of infection estimates

1. Estimates of the forces of infection for The Gambia [12]:

Age class (i)	1	2	3	4	5
Age (years)	0–1	1–5	5–10	10–15	15–80
$\lambda^g(i,t)$	0·159	0·144	0·116	0·089	0·030

Matrices of the transmission coefficients $\beta_1(i,j)$ were calculated from the forces of infection using a particular 'who acquires infection from whom' or WAIFW matrix [16]:

https://doi.org/10.1017/S0950268800003605 Published online by Cambridge University Press

(*a*) 3% population growth

*i**j*	1	2	3	4	5
1	14·13	6·80	4·42	3·11	0·84
2	6·80	6·80	4·42	3·11	0·84
3	4·42	4·42	4·42	3·11	0·84
4	3·11	3·11	3·11	3·11	0·84
5	0·84	0·84	0·84	0·84	0·84

(b) 0% population growth (type II mortality)

*i**j*	1	2	3	4	5
1	25·78	10·78	6·61	4·47	1·02
2	10·78	10·78	6·61	4·47	1·02
3	6·61	6·61	6·61	4·47	1·02
4	4·47	4·47	4·47	4·47	1·02
5	1·02	1·02	1·02	1·02	1·02

REFERENCES

1. McMahon G, Ehrlich PH, Moustafa ZA, et al. Genetic alterations in the gene encoding the major HBsAg: DNA and immunological analysis of recurrent HBsAg derived from monoclonal antibody-treated liver transplant patients. Hepatology 1992; **15**: 757–66.
2. Cariani E, Ravaggi A, Fiordalisi G, et al. Emergence of a novel HBsAg escape mutant in a liver-transplant recipient. Hepatology 1994; **20**: A307-A.
3. Cariani E, Ravaggi A, Tanzi E, et al. Emergence of hepatitis-B virus S-gene mutant in a liver-transplant recipient. J Med Virol 1995; **47**: 410–5.
4. Ngui SL, O'Connell S, Eglin RP, Heptonstall J. Low detection rate and maternal provenance of hepatitis B virus S gene mutants in cases of failed postnatal immunoprophylaxis in England and Wales. J Infect Dis 1997; **176**: 1360–5.
5. Carman WF, Zanetti AR, Karayiannis P, et al. Vaccine-induced escape mutant of hepatitis B virus. Lancet 1990; **336**: 325–9.
6. Oon CJ, Lim GK, Ye Z, et al. Molecular epidemiology of hepatitis B virus vaccine variants in Singapore. Vaccine 1995; **13**: 699–702.
7. Carman WF, Korula J, Wallace L, MacPhee R, Mimms L, Decker R. Fulminant reactivation of hepatitis B due to envelope protein mutant that escaped detection by monoclonal HBsAg ELISA. Lancet 1995; **345**: 1406–7.
8. Okamoto H, Yano K, Nozaki Y, et al. Mutations within the S gene of hepatitis B virus transmitted from mothers to babies immunized with hepatitis B immune globulin and vaccine. Pediatr Res 1992; **32**: 264–8.
9. Fortuin M, Karthigesu V, Allison L, et al. Breakthrough infections and identification of a viral variant in Gambian children immunized with hepatitis B vaccine. J Infect Dis 1994; **169**: 1374–6.
10. Ogata N, Miller RH, Ishaka KG, Zanetti AR, Purcell RH. Genetic and biological characterization of two hepatitis B variants: a precore mutant implicated in fulminant hepatitis and a surface mutant resistant to immunoprophylaxis. International Symposium on Viral Hepatitis and Liver Disease, 1994; 238–42.
11. Ghendon Y. WHO strategy for the global elimination of new cases of hepatitis B. Vaccine 1990; **8**: S134–8.
12. Edmunds WJ, Medley GF, Nokes DJ. The transmission dynamics and control of hepatitis B virus in The Gambia. Stat Med 1996; **15**: 2215–33.
13. McLean AR. Vaccination, evolution and changes in the efficacy of vaccines – a theoretical framework. Proc R Soc Lond B Biol Sci 1995; **261**: 389–93.
14. Wilson JN, Nokes DJ, Carman WF. The predicted pattern of emergence of vaccine-resistant hepatitis B: a cause for concern? Vaccine 1999; **17**: 973–8.
15. Edmunds WJ, Medley GF, Nokes DJ, Hall AJ, Whittle HC. The influence of age on the development of the hepatitis B carrier state. Proc R Soc Lond B Biol Sci 1993; **253**: 197–201.
16. Anderson RM, May RM. Infectious diseases of humans: dynamics and control. Oxford: Oxford Science Publications, 1991.
17. McLean AR, Blumberg BS. Modelling the impact of mass vaccination against hepatitis B. I. Model formulation and parameter estimation. Proc R Soc Lond B Biol Sci 1994; **256**: 7–15.
18. McLean AR, Nowak MA. Competition between zidovudine-sensitive and zidovudine-resistant strains of HIV. AIDS 1992; **6**: 71–9.
19. McLean AR, Blower SM. Imperfect vaccines and herd immunity to HIV. Proc R Soc Lond B Biol Sci 1993; **253**: 9–13.
20. Whittle HC, Maine N, Pilkington J, et al. Long-term efficacy of continuing hepatitis B vaccination in infancy in two Gambian villages. Lancet 1995; **345**: 1089–92.
21. Edmunds WJ, Medley GF, Nokes DJ. Vaccination against hepatitis B virus in highly endemic areas: waning vaccine-induced immunity and the need for booster doses. Trans R Soc Trop Med Hyg 1996; **90**: 436–40.
22. Edmunds WJ, Medley GF, Nokes DJ, O'Callaghan CJ, Whittle HC, Hall AJ. Epidemiological patterns of hepatitis B virus (HBV) in highly endemic areas. Epidemiol Infect 1996; **117**: 313–25.
23. Population and Housing Census (1983). The Republic of The Gambia, 1987.
24. Anderson RM, May RM. Age-related changes in the rate of disease transmission: implications for the design of vaccination programmes. J Hyg 1985; **94**: 365–436.
25. Edmunds WJ. The epidemiology and control of hepatitis B virus in highly endemic areas. Ph.D. thesis, Department of Biology, Imperial College, London, 1994.
26. Girones R, Miller RH. Mutation rate of the hepadnavirus genome. Virology 1989; **170**: 595–7.
27. Nowak M, May RM. Superinfection and the evolution of parasite virulence. Proc R Soc Lond B Biol Sci 1994; **255**: 81–9.
28. Andreasen V, Pugliese A. Pathogen coexistence induced by density-dependent host mortality. J Theor Biol 1995; **177**: 159–65.
29. White LJ, Cox MJ, Medley GF. Cross immunity and vaccination against multiple microparasite strains. IMA J Math Appl Med Biol 1998; **15**: 211–33.

https://doi.org/10.1017/S0950268800003605 Published online by Cambridge University Press